Chemical Science

RSC Publishing

EDGE ARTICLE

View Article Online
View Journal | View Issue

Open Access Article. Published on 02 August 2013. Downloaded on 4/9/2021 10:16:14 AM.
This article is licensed under a Creative Commons Attribution-NonCommercial 3.0 Unported Licence.

Cite this: *Chem. Sci.*, 2013, **4**, 4035

Selective carbohydrate–lectin interactions in covalent graphene- and SWCNT-based molecular recognition systems†

Maria-Eleni Ragoussi,[a] Santiago Casado,[b] Renato Ribeiro-Viana,[c] Gema de la Torre,*[a] Javier Rojo*[c] and Tomás Torres*[ab]

Received 14th May 2013
Accepted 19th July 2013

DOI: 10.1039/c3sc51352a

www.rsc.org/chemicalscience

Two new protein recognition systems have been prepared by covalent functionalization of few-layer graphene and SWCNTs with α-D-mannosyl dendrons. A glycodendron, bearing three mannose moieties on the periphery for effective interaction with the lectin, and an azido group at the focal position, has been connected, by means of a "click" chemistry reaction, to both few-layer graphene and SWCNTs endowed with terminal ethynyl groups. The specific affinity of these systems for concanavalin A was thoroughly investigated by AFM, fluorescence and UV-Vis studies. A very reliable approach was used during the AFM investigation of this kind of hybrids; namely, we were able to capture the same object before and after treatment with ConA, which allowed us to obtain reliable conclusions, in terms of selectivity of the carbohydrate–lectin interactions over the nanocarbon platforms.

Introduction

Carbon allotropes – fullerenes, carbon nanotubes and, more recently, graphene – are considered as some of the most important materials in the 21st century. For some years, carbon nanotubes, and especially single-walled carbon nanotubes (SWCNTs), were in the vanguard of research owing to their outstanding electronic and mechanical properties,[1,2] but, nowadays, graphene and graphene-based materials have surpassed them since they offer a number of fundamentally superior qualities that render them very promising for a wide range of applications, particularly in electronic devices.[3,4] The vast potential of this carbon nanomaterial has motivated its implementation into a wide array of devices.[5,6] Ideally, graphene is a single-layer material, but samples with two or more layers (*i.e.* few-layer graphene, FLG) are being investigated with equal interest.

Graphene is nowadays attracting increasing interest for the development of highly sensitive chemical[7,8] and biological sensors[9,10] due to its unique combination of several important characteristics, namely, its single-atom thickness and inherently low electrical noise that enable ultrasensitive detection of many chemical and biological molecules, including proteins.[11]

Lectins are proteins that bind mono- and oligosaccharides with high specificity, and play an important role in biological recognition events.[12] Carbohydrate–lectin interactions are a crucial step in many biological processes, such as inflammation, embryogenesis, cell development, tumor progression, *etc.*[13] Carbohydrate–lectin binding has dissociation constants in the millimolar range, thus, multivalent systems are required for efficient recognition (simultaneous binding of multiple ligands on to multiple receptors).[14–16] In an effort to understand and mimic these biological phenomena, the preparation of multivalent systems, in which various copies of the carbohydrate ligand are present, is hence essential.

In recent years, there has been a plethora of systems reported for the investigation of carbohydrate–lectin interactions.[17–20] Among them, sugar-functionalized CNTs have received considerable attention, in non-covalent[21–26] as well as covalent systems,[21,27–30] since they are ideal platforms for the construction of multivalent architectures.[27,28] In the case of graphene-based ensembles, however, examples are scarce. To the best of our knowledge, only two non-covalent systems have been reported,[22,31] and regarding covalent approaches, no systems have been developed to date. Besides that, non-modified few layer graphene obtained by solvent assisted exfoliation of graphite[32,33] has never been used for the construction of molecular recognition systems.

Taking advantage of our broad experience in functionalizing CNTs[34,35] and graphene[33] with electroactive moieties in the search for hybrid systems for electronic applications, as well as

[a]*Departamento de Química Orgánica, Universidad Autónoma de Madrid, 28049 Madrid, Spain. E-mail: tomas.torres@uam.es; Fax: +34 9 1497 3966; Tel: +34 9 1497 4151*

[b]*IMDEA-Nanociencia, c/Faraday 9, Campus de Cantoblanco, 28049 Madrid, Spain*

[c]*Glycosystems Laboratory, Instituto de Investigaciones Químicas (IIQ) CSIC – Universidad de Sevilla Americo Vespucio, 49, 41092 Sevilla, Spain. E-mail: javier.rojo@iiq.csic.es; Fax: +34 954460165; Tel: +34 954489568*

† Electronic supplementary information (ESI) available: Synthetic procedure followed for glycodendron **5**, photos of dispersions of the graphene-based materials **8** and **9**, ^{1}H NMR spectrum of graphene–dendron hybrid **9** and AFM images of functionalized SWCNTs and FLG before and after their interaction with ConA. See DOI: 10.1039/c3sc51352a

Open Access Article. Published on 02 August 2013. Downloaded on 4/9/2021 10:16:14 AM.
This article is licensed under a Creative Commons Attribution-NonCommercial 3.0 Unported Licence.

of our background in the study of carbohydrate-based molecular recognition systems,[36–38] we have prepared novel hybrids for the investigation of carbohydrate–lectin interactions. We, thus, describe herein a new molecular recognition system based on non-modified graphene, as well as a related SWCNT-based ensemble, covalently linked to mannose–glycodendrons. We opted for the covalent instead of supramolecular binding of our carbohydrate ligands to the surface of the nanocarbon materials, taking into consideration the major advantages of this approach, namely, greater stability of the hybrid material, control over the degree of functionalization, and reproducibility. The specific affinity of these systems for concanavalin A (ConA) was thoroughly investigated as a proof of concept to demonstrate the viability of these platforms for bio-sensing applications.

Results and discussion

We have used a glycodendron bearing three mannose moieties on the periphery, for effective interaction with the lectin, and an azido group at the focal position for carrying out a "click" chemistry reaction to connect it to carbon nanostructures endowed with terminal ethynyl groups. The synthesis of glycodendron **5** was achieved in four steps, starting from pentaerythritol, by a procedure described in the literature (Scheme S1 in the ESI†).[36,39] Briefly, the trialkynylated compound **1** was prepared from commercially available pentaerythritol by reaction with propargyl bromide and sodium hydride. Then, a short, conveniently functionalized spacer was conjugated to the fourth hydroxyl group giving rise to compound **2**. The mannosyl units were incorporated to the core by means of Cu(I) catalyzed azide–alkyne cycloaddition (CuAAC), using mannosyl derivative **3** previously synthesized in our group[40] to yield trivalent dendron **4**. Finally, substitution of the chloro by an azido group provided compound **5**, ready to be clicked on the conveniently functionalized surfaces.

At the same time, graphene, and also SWCNTs were initially functionalized with a phenylethynyl group, to install the required alkyne for the CuAAC reaction. In the case of SWCNTs, microwave irradiation of a well-dispersed batch of carbon nanotubes in *o*-DCB, in the presence of isoamyl nitrite and 4-[(trimethylsilyl)ethynyl]aniline,[41] afforded derivative **6** (Scheme 1). Thermogravimetric analysis (TGA) showed that microwave irradiation led to a significantly higher degree of functionalization when compared to thermal conditions previously used by us (Fig. 1a).[34] More specifically, the number of phenylacetylene groups in **6** were estimated to be 1 per 70 carbon atoms at 600 °C (17% weight loss), more than double of what we had previously achieved (8%). In addition, a much lower reaction time, 1.5 instead of 48 h, was required. Derivative **6** was subsequently treated with TBAF to remove the protecting TMS group and was then immediately subjected to a Cu(I)-catalyzed 1,3-dipolar cycloaddition with trivalent dendron **5**, to afford final hybrid **7** (Scheme 1). Taking into consideration the total decomposition of **5** at 600 °C (86%), an average functionalization of 1 glycodendron per *ca.* 170 carbon atoms (35% weight loss) was calculated (Fig. 1a). It is noteworthy that the additional weight loss of hybrid **7** with respect to that of phenylethynyl–SWCNT precursor **6** was detected at a temperature above 300 °C, which matches the weight loss temperature of the mannosyl dendron **5** (Fig. 1a), that being strong evidence for the linkage of the dendron to the carbon nanostructure.

Regarding glycographene system **9**, its preparation differed slightly to that described above, since the first step involved exfoliation of graphite to obtain FLG, using the well-known method of liquid exfoliation in NMP.[32,33] The suspension of FLG was immediately subjected to microwave irradiation to install the necessary alkyne, and was followed by deprotection and "click" reaction to link the carbohydrate dendron (Scheme 1). TGA experiments revealed that a significantly lower degree of functionalization was achieved, when compared to SWCNT-based hybrid **7**, which was expected considering the minor reactivity of this carbon nanomaterial. In particular, we calculated 9% weight loss at the initial functionalization step (hybrid **8**), which corresponds to 1 phenylacetylene group per *ca.* 150 carbon atoms. After implementation of the sugars, an extra 6% weight loss (when considering the total decomposition of **5** at 600 °C) was observed, corresponding to 1 glycodendron per *ca.* 1500 carbon atoms (Fig. 1b).

The solubility/dispersability of SWCNT- and graphene-glycodendron hybrids **7** and **9** was tested in various solvents. Even though water solubility is desirable for biological applications, the attachment of mannose-based dendrons does not lead to water-soluble materials. Nevertheless, nanoconjugate **9** forms very stable suspensions in DMSO (Fig. S1 in ESI†) which remain stable after five days, whereas those of both protected graphene–phenylethynyl system **8** and exfoliated graphene show a black precipitate after that period of time. The stability and homogeneity of the dispersions of **9** allowed us to carry out ^{1}H NMR experiments in DMSO-d_6. From the spectrum (Fig. S2 in ESI†) we obtained irrefutable proof for the covalent linkage of the glycodendron to the modified graphene surface, since a new singlet appeared at 8.31 ppm, which corresponds to the proton of the triazole ring formed in the latter "click" chemistry reaction between phenylethynyl-functionalized graphene precursor **8** and glycodendron **5**. This signal integrates perfectly with the signal at 7.95 ppm (1 : 3 ratio), which corresponds to the pre-existing triazole rings of the glycodendron (Fig. S2 in ESI†). Unfortunately, the quality of the dispersions of the related SWCNT-based hybrid **7** in different solvents was too low to perform NMR characterization of this material.

With the two new systems (*i.e.* **7** and **9**) in hand, we proceeded to the study of their interaction with a lectin that selectively binds mannose. Among lectins, the most widely used in affinity studies is the commercially available concanavalin A (ConA) from *Canavalia ensiformis* (purified from jack-bean). ConA is a tetrameric lectin (at pH 7.0 or above) that selectively binds mannose and glucose. For maintaining the loop-type active conformation and establishing effective sugar-binding activity, it requires the presence of divalent cations, most specifically, calcium and/or manganese.[42]

Atomic force microscopy (AFM) was the tool we used to obtain initial proof for the successful functionalization of the carbon nanostructures with glycoconjugate **5**, and then for the

 This journal is © The Royal Society of Chemistry 2013

Open Access Article. Published on 02 August 2013. Downloaded on 4/9/2021 10:16:14 AM.
This article is licensed under a Creative Commons Attribution-NonCommercial 3.0 Unported Licence.

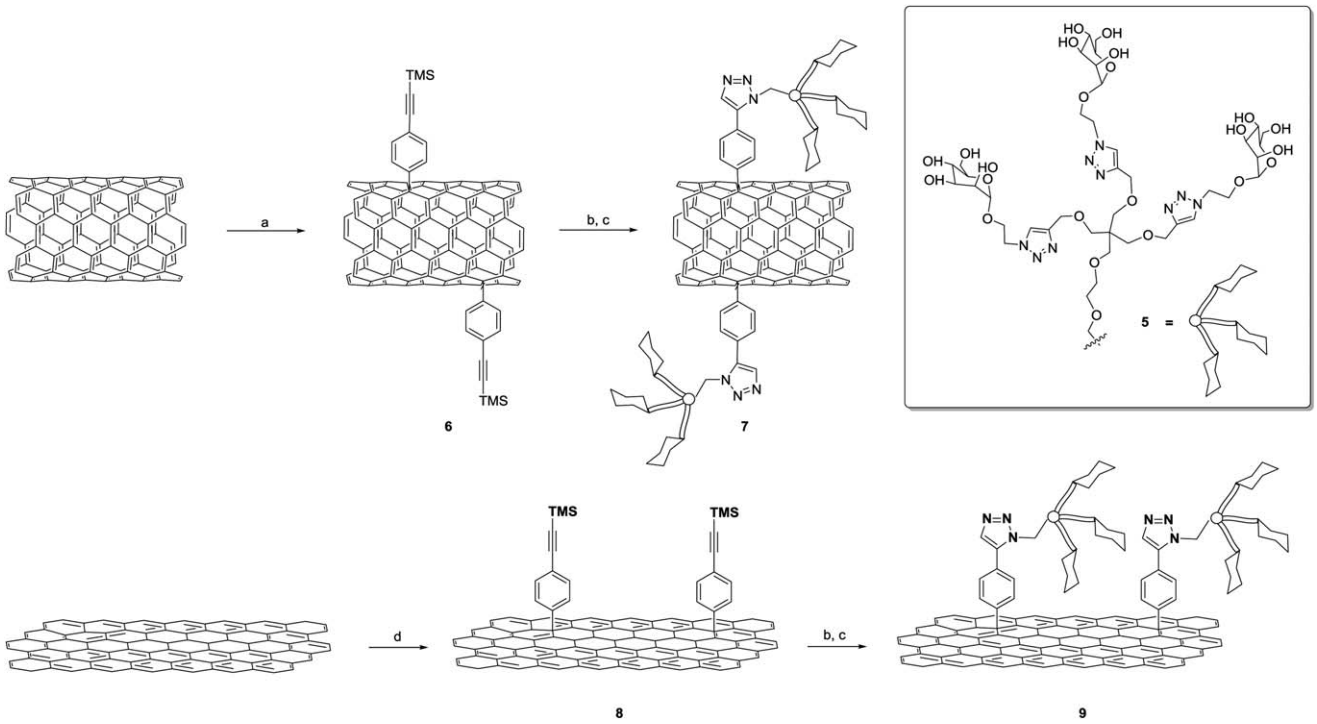

Scheme 1 *Reagents and conditions*: (a) 4-[(trimethylsilyl)ethynyl]aniline, isoamyl nitrite, *o*-DCB, MW, 80 °C, 1.5 h; (b) TBAF, 0 °C to rt, 2 h; (c) dendron **5**, $CuSO_4$, sodium ascorbate, 70 °C, 48 h; (d) 4-[(trimethylsilyl)ethynyl]aniline, isoamyl nitrite, NMP, MW, 80 °C, 1.5 h.

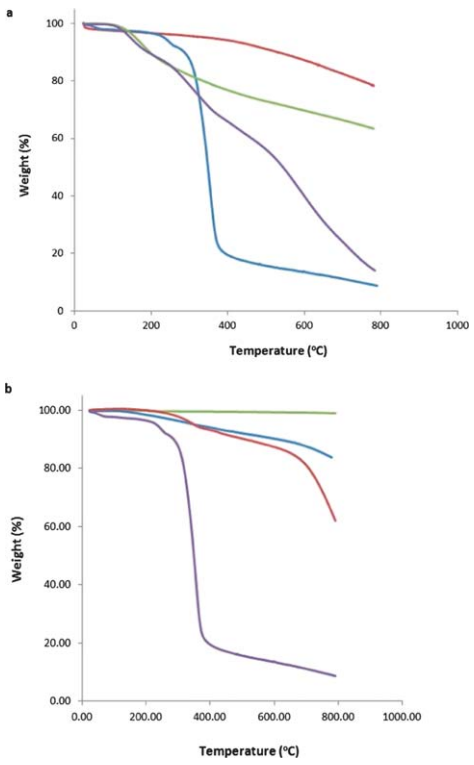

Fig. 1 TGA for (a) SWCNT-based hybrids (red line: pristine SWCNTs, green line: conjugate **6**, purple line: conjugate **7**, blue line: glycodendron **5**) and (b) graphene-based hybrids (green line: exfoliated graphene, blue line: conjugate **8**, red line: conjugate **9**, purple line: glycodendron **5**).

selective interaction of the hybrids with ConA. All measurements were performed on poly-lysine treated mica surfaces, this treatment allowing the carbon nanostructures to stick robustly to the surface.

Concerning SWCNTs, as shown in Fig. 2a, a height of approximately 1 nm was measured for derivative **6**, bearing the alkyne moieties. After installing the mannose glycoconjugates,

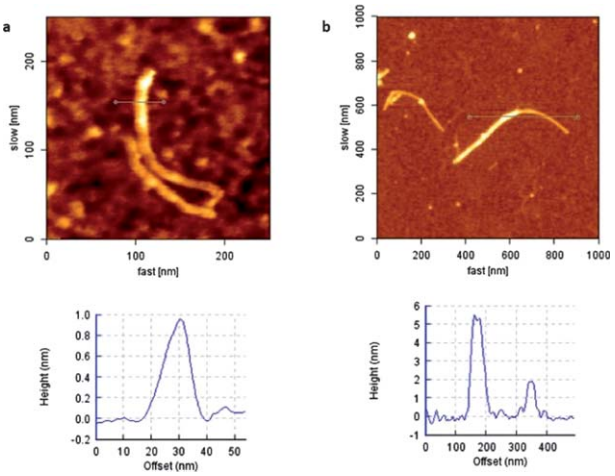

Fig. 2 (a) SWCNT before installation of carbohydrate dendron (**6**) and height profile and (b) SWCNT after installation of carbohydrate dendron (**7**) and height profile. Please note that the highest profile (*ca.* 5 nm) would correspond to the location of dendritic units in the "lower" and in the "upper" positions of the tube; and the lowest profile (2 nm) would correspond to a region where no dendrons are attached to the top.

Open Access Article. Published on 02 August 2013. Downloaded on 4/9/2021 10:16:14 AM.
This article is licensed under a Creative Commons Attribution-NonCommercial 3.0 Unported Licence.

the height was raised to *ca.* 5 nm (Fig. 2b). In addition, zooming into one nanotube (Fig. S3a in ESI†), we could observe higher and lower parts, which can be attributed to the dendron being randomly implemented around the nanotube, where the alkynes were originally installed, as already demonstrated by ^{1}H NMR (Fig. S2 in ESI†). The estimated length of the glycodendron excluding the ethyleneglycol linker is 1.5 nm.[36] Considering that the dendron units can be randomly located along the whole nanotube, namely in the lower part stuck to the surface and also in the upper part, the observed increase fits quite well with that expected for these systems. Similarly, imaging a sample of FLG bearing the alkyne groups, the height was of the order of 4–8 nm, whereas in hybrid **9** there was an average increase of around 6–8 nm (Fig. S3b and c in ESI†). In this case, the calculated increase in height after installation of the dendron does not necessarily fit with the observed value, considering that each flake imaged may have a different number of layers. It should also be pointed out that the relatively large height values found for the FLG are consistent, not only with the presence of several graphene layers, but also with the presence of glycodendron protuberances which do not allow for a fully planar deposition of the graphene flakes on the substrate even if the functionalization is only random along the surface.

At this point, for the investigation of the affinity of SWCNT– and graphene–carbohydrate hybrids with ConA, we adopted a reliable strategy for measuring this selective interaction. In contrast to other works reported so far, we imaged the exact same CNT or graphene item before and after treatment with ConA. Focusing on the same nanotube or flake and measuring the height at the same position before and after the interaction with the lectin, the evidence of sugar–protein recognition is much more accurate.

Hence, we set off our interaction studies by drop-casting an ethanol dispersion of graphene-hybrid **9** to a poly-lysine-treated mica surface, and obtained an image of one FLG flake (Fig. 3a and Fig. S4 in ESI†) with a height of around 10 nm. Maintaining the area of measurement, we incubated the surface with a 0.2 mg mL^{-1} solution of ConA in phosphate buffered saline (PBS), in the presence of either Mn^{2+} or Ca^{2+} ions, for 45 min. It should be pointed out that Mn^{2+} ions augment the lectin–carbohydrate interaction compared to Ca^{2+}, as stated in a recent report[17] and indeed, incubation in the presence of Ca^{2+} did not afford conclusive results. Hence, we continued our studies using Mn^{2+}. We took images in the presence of the lectin solution (Fig. 3b and S4 in ESI†) because, in this way, we could avoid ConA aggregates on the mica, as well as on the FLG flakes, which could cause difficulties and inaccuracies in the study of the selective interaction process. Under these conditions, an increase in height of *ca.* 10 nm was observed. The size of ConA at pH 7 or higher, as determined by X-ray diffraction studies, is 60 × 70 × 70 Å. Although the height increase of the FLG flake is somewhat larger than the size of ConA, the measured value fully fits with that previously reported for graphene materials non-covalently linked to related glycoconjugates, which interact with ConA.[22] To demonstrate that a selective binding with the mannose moieties is taking place, we performed a control

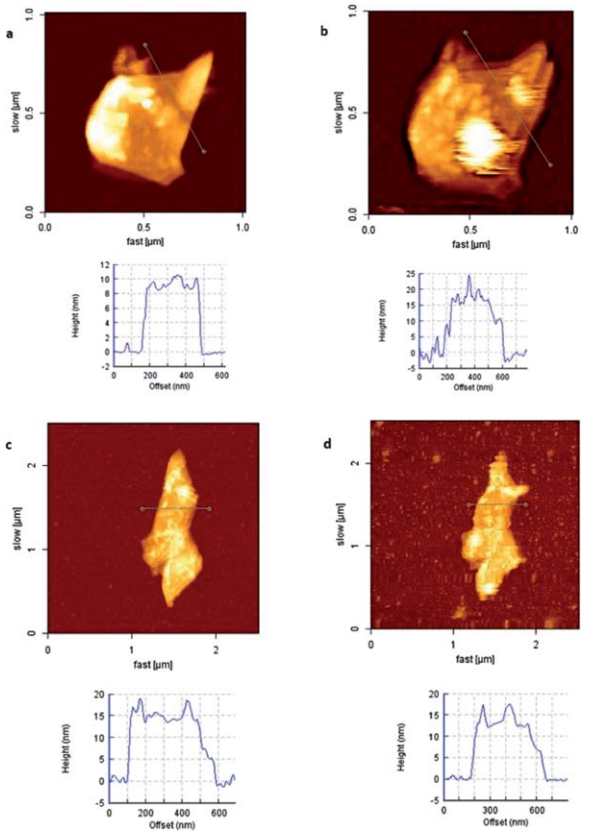

Fig. 3 (a) Graphene–carbohydrate **9** before incubation with ConA and height profile, (b) graphene–carbohydrate **9** after incubation with ConA for 45 min, and height profile, (c) graphene–carbohydrate **9** before incubation with BSA and height profile, and (d) graphene–carbohydrate **9** after incubation with BSA for 45 min and height profile.

experiment with non-specific protein, BSA (albumin from bovine serum). By the same procedure, focusing on one FLG flake, we carried out the incubation of the mica surface with a solution of BSA at the same concentration (*i.e.* 0.2 mg mL^{-1}) in PBS in the presence of Mn^{2+} and then measured the same flake again. As assumed, no significant change in height was observed in this case (Fig. 3c and d). This observation proved the selectivity of our system and also allowed us to discard that the height differences observed in the experiment with ConA were a consequence of roughness differences on the background due to direct ConA unspecific adhesion to the treated mica.

For the nanotube-based systems, the same sequence of experiments was applied. After drop-casting an ethanol dispersion of SWCNT-hybrid **7** to a treated mica surface, we followed the height changes on some selected nanotubes (Fig. 4a and S5 in ESI†) with a height of 4 nm at their highest part. In this case, we could not take well-resolved images of the nanotubes in the presence of the lectin solution, probably because their interaction with the treated surface is lower in these conditions. This could be a consequence of the lower number of contact points when compared to FLG flakes, which are more planar and less functionalized (see the functionalization degree obtained by TGA measurements).

 This journal is © The Royal Society of Chemistry 2013

Open Access Article. Published on 02 August 2013. Downloaded on 4/9/2021 10:16:14 AM.
This article is licensed under a Creative Commons Attribution-NonCommercial 3.0 Unported Licence.

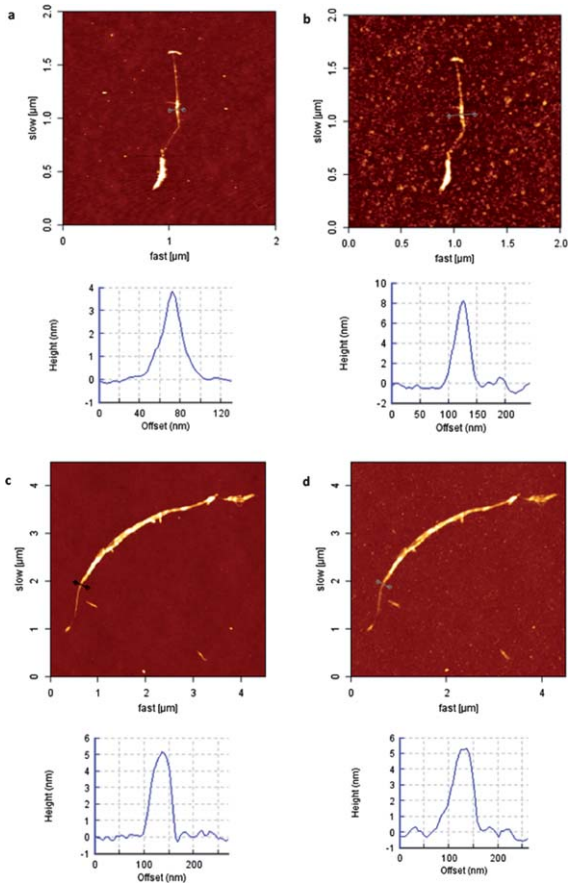

Fig. 4 (a) SWCNT–carbohydrate **7** before incubation with ConA and height profile, (b) SWCNT–carbohydrate **7** after incubation with ConA for 45 min and height profile, (c) SWCNT–carbohydrate **7** before incubation with BSA and height profile, and (d) SWCNT–carbohydrate **7** after incubation with BSA for 45 min and height profile.

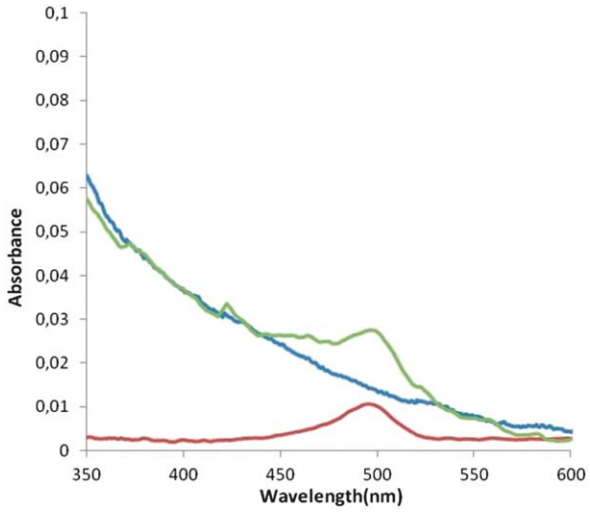

Fig. 5 UV-Vis spectrum of ConA-Alexa488 in PBS (red line), SWCNT-glyco-conjugate **7** incubated in ConA-Alexa488 in PBS (green line) and bare SWCNT incubated in ConA-Alexa488 in PBS (blue line).

Thus, imaging of the nanotubes was carried out in air. In particular, after incubation and subsequent washing with water to remove excess lectin, we captured images of the exact same nanotube (Fig. 4b and S5b in ESI†). An increase in height of 4 nm was observed in the swollen parts of the nanotube (Fig. 4b and S5b in ESI†), whilst the thinner parts remained unaltered (Fig. S5c and d in ESI†). The increase in height fully fits, in this case, with the ConA dimensions. Finally, a reference experiment with BSA was also conducted for SWCNT-hybrid **7**, and once again, no change in height was observed, as demonstrated in Fig. 4c and d.

To further corroborate the affinity of our systems for ConA, we decided to perform fluorescence and UV-Vis experiments using fluorescently labeled lectin ConA-Alexa488. In particular, fluorescence evaluation was not possible for FLG nanohybrid **9** due to the well-known fluorescence-quenching effect of graphene,[43] and only UV-vis spectra over dispersions of this material could be performed (see below). To conjugate ConA with hybrid systems **7** and **9**, fine dispersions of the nanoconjugates in EtOH/PBS were treated with a solution of ConA-Alexa488 in PBS and incubated for 1 h. Centrifugation and washing with PBS, to remove excess of the lectin, afforded the modified materials, in which the fluorescent lectin would be fixed at the mannose residues. Fluorescence and AFM coupled images of dispersions of the fluorescent-ConA-treated SWCNT-hybrid **7** on mica are depicted in Fig. S6 in ESI.† The fluorescence image displays some fluorescent spots in the same positions as the bundles of nanotubes in the AFM image. This observation confirms the preference of the lectin for the modified nanotube, since no trace of fluorescence could be observed in the rest of the surface. In addition, UV-Vis experiments over dispersions of the modified hybrid **7** in PBS showed the signature of the fluorescent ConA at 490 nm (Fig. 5). In contrast, when incubating pristine SWCNTs with ConA, no apparent trace of the fluorescent lectin was observed. Similarly, the interaction of graphene-conjugate **9** with fluorescent ConA is clearly visible in the UV-vis spectrum of the fluorescent-ConA-treated hybrid **9**, whereas no interaction was observed when non-functionalized, exfoliated graphene was incubated with the lectin (Fig. S7 in ESI†).

Conclusions

In conclusion, we have prepared two new FLG- and SWCNT-based protein recognition systems, by covalent functionalization with trivalent α-D-mannosyl dendrons. These systems demonstrated selective interaction with ConA, as proved by AFM, fluorescence and UV-Vis studies. The key features of this work rely on three crucial points. First, the covalent linkage of the glycodendrons to the nanocarbon materials afforded novel and robust systems for this type of studies. Second, this is the first report on non-modified graphene being used for functionalization with carbohydrates and biological studies. And, lastly, a novel approach was used during the AFM investigation of this kind of hybrids, namely, we succeeded in capturing the same object before and after treatment with ConA, which allowed us to obtain highly reliable results, in terms of

Open Access Article. Published on 02 August 2013. Downloaded on 4/9/2021 10:16:14 AM. This article is licensed under a Creative Commons Attribution-NonCommercial 3.0 Unported Licence.

selectivity of carbohydrate–lectin interactions over the nanocarbon platforms. Concerning future applications of the herein described architectures, they show high potential for their incorporation in biosensors, as well as drug-delivery systems.

Experimental

General

^{1}H NMR spectra were recorded at 300 MHz at 25 °C with a BRUKER AC-300 instrument. UV-Vis spectra were recorded with a JASCO V-660 spectrophotometer. Thermogravimetric analyses were performed with a thermobalance TGA Q500 TA Instrument equipped with an EGA oven at 10 °C min^{-1} under N_2 (90 mL min^{-1} flux). Atomic force microscopy (AFM) characterization was performed using a JPK NanoWizard II, coupled to a Nikon Eclipse Ti inverted fluorescence optical microscope. An Olympus commercial silicon nitride cantilever tip (OMCL-RC800PSA) with a force constant of 0.76 N m^{-1} and a resonant frequency of 71 kHz was employed in dynamic mode.

Materials

Graphite flakes (+100 mesh, ≥75% min) were purchased from Aldrich, as well as all other chemicals, except HiPco SWCNTs, purchased from Carbon Nanotechnologies Inc., and fluorescent ConA from Invitrogen.

Preparation of AFM samples

Freshly peeled mica was submerged in a 0.001% poly-lysine solution for 1 min, then rinsed with water and dried with Ar. A dispersion of the graphene sample in EtOH was then drop-casted onto the coated mica. After evaporation of the solvent, the samples were investigated. For the incubation with specific and non-specific lectins, a solution of the corresponding lectin (c = 0.2 mg mL^{-1}) in PBS in the presence of $MnBr_2$ (c = 1 mg mL^{-1}) was drop-casted on the mica surface and incubated for 45 min. In the case of the SWCNTs, after incubation the mica surface was washed with water and dried in air.

Synthesis

SWCNT–phenylacetylene (6). Pristine SWCNTs (5 mg) were dispersed in *o*-DCB (15 mL) and a solution of 4-[(trimethylsilyl)-ethynyl]aniline (230 mg, 1.22 mmol) was added. Then isoamyl nitrite was added (0.1 mL followed by another 0.1 mL for the second round of irradiation) and the mixture was subjected to microwave irradiation (100 W, 80 °C, 30 min followed by 30 W, 80 °C, 1 h). It was then brought to room temperature, filtered through a PTFE membrane and washed with deionized water, MeOH, acetone and CH_2Cl_2, to afford hybrid **6**.

SWCNT–carbohydrate (7). To a suspension of SWCNT–phenylacetylene **6** (5 mg) in NMP (10 mL) at 0 °C was added a solution of tetrabutylammonium fluoride (1 M in THF) (2 mL). The reaction mixture was stirred at room temperature for 2 h then filtered on a PTFE membrane and washed several times with DMF and then with CH_2Cl_2. It was then redissolved in NMP and mannosyl dendron **5** (7 mg, 0.006 mmol), $CuSO_4 \cdot 5H_2O$ (0.8 mg, 0.003 mmol) and sodium ascorbate (6.2 mg, 0.03 mmol) were added. The reaction mixture was stirred at 70 °C for 48 h and then filtered on a PTFE membrane. In order to remove sodium ascorbate, copper catalyst and free mannosyl dendron, the black solid was sonicated and washed with mixtures of DMF–water (v/v 1/4) and DMF–THF (v/v 1/4) and then filtered. The solid was finally washed with THF and CH_2Cl_2, to afford hybrid **7**.

Graphene–phenylacetylene (8). Exfoliated graphene (5 mg) was dispersed in NMP (8 mL) and a solution of 4-[(trimethylsilyl)ethynyl]aniline (300 mg, 1.58 mmol) was added. Then, isoamyl nitrite was added (0.1 mL followed by another 0.1 mL for the second round of irradiation) and the mixture was subjected to microwave irradiation (100 W, 80 °C, 30 min followed by 30 W, 80 °C, 1 h). It was then brought to room temperature, filtered through a PTFE membrane and washed with deionized water, MeOH, acetone and CH_2Cl_2, to afford hybrid **8**.

Graphene–carbohydrate (9). To a suspension of graphene–phenylacetylene **8** (5 mg) in NMP (10 mL) at 0 °C was added a solution of tetrabutylammonium fluoride (1 M in THF) (2 mL). The reaction mixture was stirred at room temperature for 2 h then filtered on a PTFE membrane and washed several times with DMF and then with CH_2Cl_2. It was then redissolved in NMP and mannosyl dendron **5** (7 mg, 0.006 mmol), $CuSO_4 \cdot 5H_2O$ (0.8 mg, 0.003 mmol) and sodium ascorbate (6.2 mg, 0.03 mmol) were added. The reaction mixture was stirred at 70 °C for 48 h and then filtered on a PTFE membrane. In order to remove sodium ascorbate, copper catalyst and free mannosyl dendron, the black solid was sonicated and washed with mixtures of DMF–water (v/v 1/4) and DMF–THF (v/v 1/4) and then filtered. The solid was finally washed with THF and CH_2Cl_2, to afford hybrid **9**.

Acknowledgements

Financial support is acknowledged from the Spanish MICINN (CTQ2011-24187/BQU, CTQ2011-23410/BQU and CONSOLIDER INGENIO 2010, CSD2007-00010 on Molecular Nanoscience) and the Comunidad de Madrid (MADRISOLAR-2, S2009/PPQ/1533). Thanks to the subscription of Red de Bibliotecas del CSIC to the RSC Gold for Gold Application for getting open access for this article.

Notes and references

1 S. Reich, C. Thomsen and J. Maultzsh, *Carbon Nanotubes: Basic Concepts and Physical Properties*, VCH, Weinheim, 2004.
2 V. Sgobba and D. M. Guldi, *Chem. Soc. Rev.*, 2009, **38**, 165.
3 M. J. Allen, V. C. Tung and R. B. Kaner, *Chem. Rev.*, 2010, **110**, 132.
4 X. Huang, X. Qi, F. Boey and H. Zhang, *Chem. Soc. Rev.*, 2012, **41**, 666.
5 N. O. Weiss, H. Zhou, L. Liao, Y. Liu, S. Jiang, Y. Huang and X. Duan, *Adv. Mater.*, 2012, **24**, 5782.
6 X. Huang, Z. Zeng, Z. Fan, J. Liu and H. Zhang, *Adv. Mater.*, 2012, **24**, 5979.
7 K. R. Ratinac, W. Yang, S. P. Ringer and F. Braet, *Environ. Sci. Technol.*, 2010, **44**, 1167.

 This journal is © The Royal Society of Chemistry 2013

Open Access Article. Published on 02 August 2013. Downloaded on 4/9/2021 10:16:14 AM.
This article is licensed under a Creative Commons Attribution-NonCommercial 3.0 Unported Licence.

8 F. Schedin, A. K. Geim, S. V. Morozov, E. W. Hill, P. Blake, M. I. Katsnelson and K. S. Novoselov, *Nat. Mater.*, 2007, **6**, 652.
9 H. Jiang, *Small*, 2011, **7**, 2413.
10 Y. Liu, X. Dong and P. Chen, *Chem. Soc. Rev.*, 2012, **41**, 2283.
11 S. Mao, G. Lu, K. Yu, Z. Bo and J. Chen, *Adv. Mater.*, 2010, **22**, 3521.
12 H. Lis and N. Sharon, *Chem. Rev.*, 1998, **98**, 637.
13 C. R. Bertozzi and L. L. Kiessling, *Science*, 2001, **291**, 2357.
14 M. Mammen, S.-K. Choi and G. M. Whitesides, *Angew. Chem., Int. Ed.*, 1998, **37**, 2754.
15 Y. C. Lee and R. T. Lee, *Acc. Chem. Res.*, 1995, **28**, 321.
16 P. I. Kitov and D. R. Bundle, *J. Am. Chem. Soc.*, 2003, **125**, 16271.
17 B. K. Gorityala, Z. Lu, M. L. Leow, J. Ma and X. W. Liu, *J. Am. Chem. Soc.*, 2012, **134**, 15229.
18 J.-F. Nierengarten, J. Iehl, V. Oerthel, M. Holler, B. M. Illescas, A. Muñoz, N. Martín, J. Rojo, M. Sánchez-Navarro, S. Cecioni, S. Vidal, K. Buffet, M. Durka and S. P. Vincent, *Chem. Commun.*, 2010, **46**, 3860.
19 N. Jayaraman, *Chem. Soc. Rev.*, 2009, **38**, 3463.
20 B. T. Houseman and M. Mrksich, *Top. Curr. Chem.*, 2002, **218**, 1.
21 Y. Chen, A. Star and S. Vidal, *Chem. Soc. Rev.*, 2013, **42**, 4532.
22 Y. Chen, H. Vedala, G. P. Kotchey, A. Audfray, S. Cecioni, A. Imberty, S. Vidal and A. Star, *ACS Nano*, 2012, **6**, 760.
23 H. Vedala, Y. Chen, S. Cecioni, A. Imberty, S. Vidal and A. Star, *Nano Lett.*, 2011, **11**, 170.
24 T. Hasegawa, T. Fujisawa, M. Numata, M. Umeda, T. Matsumoto, T. Kimura, S. Okumura, K. Sakurai and S. Shinkai, *Chem. Commun.*, 2004, 2150.
25 N. Khiar, M. P. Leal, R. Baati, C. Ruhlmann, C. Mioskowski, P. Schultz and I. Fernandez, *Chem. Commun.*, 2009, 4121.
26 K. S. Vasu, K. Naresh, R. S. Bagul, N. Jayaraman and A. K. Sood, *Appl. Phys. Lett.*, 2012, **101**, 053701.
27 P. G. Luo, H. Wang, L. Gu, F. Lu, Y. Lin, K. A. Christensen, S. T. Yang and Y. P. Sun, *ACS Nano*, 2009, **3**, 3909.
28 L. Gu, T. Elkin, X. Jiang, H. Li, Y. Lin, L. Qu, T.-R. J. Tzeng, R. Joseph and Y.-P. Sun, *Chem. Commun.*, 2005, 874.
29 H. Wang, L. Gu, Y. Lin, F. Lu, M.-J. Meziani, P.-G. Luo, W. Wang, L. Cao and Y.-P. Sun, *J. Am. Chem. Soc.*, 2006, **128**, 13364.
30 C. Gao, S. Muthukrishnan, W. Li, J. Yuan, Y. Xu and A. H. E. Muller, *Macromolecules*, 2007, **40**, 1803.
31 Q. Chen, W. Wei and J.-M. Lin, *Biosens. Bioelectron.*, 2011, **26**, 4497.
32 Y. Hernandez, V. Nicolosi, M. Lotya, F. M. Blighe, Z. Sun, S. De, I. T. McGovern, B. Holland, M. Byrne, Y. K. Gun'Ko, J. J. Boland, P. Niraj, G. Duesberg, S. Krishnamurthy, R. Goodhue, J. Hutchison, V. Scardaci, A. C. Ferrari and J. N. Coleman, *Nat. Nanotechnol.*, 2008, **3**, 563.
33 M.-E. Ragoussi, J. Malig, G. Katsukis, B. Butz, E. Spiecker, G. de la Torre, T. Torres and D. M. Guldi, *Angew. Chem., Int. Ed.*, 2012, **51**, 6421.
34 S. Campidelli, B. Ballesteros, A. Filoramo, D. Diaz Diaz, G. de la Torre, T. Torres, G. M. Aminur Rahman, C. Ehli, D. Kiessling, F. Werner, V. Sgobba, D. M. Guldi, C. Cioffi, M. Prato and J.-P. Bourgoin, *J. Am. Chem. Soc.*, 2008, **130**, 11503.
35 B. Ballesteros, G. de la Torre, C. Ehli, G. M. A. Rahman, F. Agulló-Rueda, D. M. Guldi and T. Torres, *J. Am. Chem. Soc.*, 2007, **129**, 5061.
36 R. Ribeiro-Viana, M. Sánchez-Navarro, J. Luczkowiak, J. R. Koeppe, R. Delgado, J. Rojo and B. G. Davis, *Nat. Commun.*, 2012, **3**, 1303.
37 J. Luczkowiak, A. Muñoz, M. Sánchez-Navarro, R. Ribeiro-Viana, A. Ginieis, B. M. Illescas, N. Martín, R. Delgado and J. Rojo, *Biomacromolecules*, 2013, **14**, 431.
38 M. Sánchez-Navarro, A. Muñoz, B. M. Illescas, J. Rojo and N. Martín, *Chem.–Eur. J.*, 2011, **17**, 766.
39 M. Ortega-Muñoz, J. Lopez-Jaramillo, F. Hernandez-Mateo and F. Santoyo-Gonzalez, *Adv. Synth. Catal.*, 2006, **348**, 2410.
40 E. Arce, P. M. Nieto, V. Díaz, R. G. Castro, A. Bernad and J. Rojo, *Bioconjugate Chem.*, 2003, **14**, 817.
41 J.-J. Hwang and J. M. Tour, *Tetrahedron*, 2002, **58**, 10387.
42 K. D. Hardman and C. F. Ainsworth, *Biochemistry*, 1972, **11**, 4910.
43 K. P. Loh, Q. Bao, G. Eda and M. Chhowalla, *Nat. Chem.*, 2010, **2**, 1015.